2008

Radiation View Factors Between a Disk and the Interior of a Class of Axisymmetric Bodies Including Converging Diverging Rocket Nozzles

Mark Richard Murad
Cleveland State University

RADIATION VIEW FACTORS BETWEEN A DISK AND THE INTERIOR OF A CLASS OF AXISYMMETRIC BODIES INCLUDING CONVERGING DIVERGING ROCKET NOZZLES

MARK RICHARD MURAD

Bachelor of Science in Mechanical Engineering

Cleveland State University

May, 1994

Bachelor of Science in Chemical Engineering

Cleveland State University

May, 1994

submitted in partial fulfillment of the requirements for the degree

MASTERS OF SCIENCE IN MECHANICAL ENGINEERING

at the

CLEVELAND STATE UNIVERSITY

May 2008

This thesis has been approved for the

Department of **MECHANICAL ENGINEERING**

and the College of Graduate Studies by

Thesis Committee Chairperson, Dr. Ebiana

Department/Date

Dr. Rashidi

Department/Date

Dr. Frater

Department/Date

Dr. Oprea

Department/Date

To God the Father the Son and the Holy Spirit, ...

ACKNOWLEDGMENTS

The author would like to dedicate this work to Dr. Benjamin T. F. Chung for all of his invaluable teaching skills in training the author in his Heat Transfer Discipline. The author would also like to acknowledge the fact that Dr. Chung was the teacher of several of the authors undergraduate schools teachers in the authors dual Chemical and Mechanical Engineering disciplines. Very rare in life does someone have the privilege to be taught by your Undergraduate schools teachers, Graduate schoolteacher.Dr. Mohammad Hossien N. Naraghi helped with the rocket nozzle view factors.

The author would also like to thank Dr. Asuquo Ebiana for allowing the author to pursue the subject as his thesis at Cleveland State University. Dr. John Oprea for all of his Differential Geometry and his mathematical teaching expertise, patience and Maple programs and graphics that allowed me to derive the equations presented in this thesis. Dr. Majid Rashdi, Dr. John Frater, Dr. William Atherton for all of his help with getting this thesis done. Dr. Nagamanth Sridhar for all his help in Latex, Mike Holstein for all his help in Unix and Linux conversion from Mathematica and Maple on the Ohio SuperComputer. Mike Somos for all of his help in Mathematica and Tex, Dr. Richter for all his help in Latex. Dr. Stuart Clary for all his help in Mathematica. Dr. Dennis Schneider and Ed Boss Mathematica trainers. David Gurarie with his help in nonlinear partial differential equation modeling. "This work was supported in part by an allocation of computing time from the Ohio Supercomputer Center."

RADIATION VIEW FACTORS BETWEEN A DISK AND THE INTERIOR OF A CLASS OF AXISYMMETRIC BODIES INCLUDING CONVERGING DIVERGING ROCKET NOZZLES

MARK RICHARD MURAD

ABSTRACT

A general symbolic exact analytic solution is developed for the radiation view factors including shadowing by the throat between a divergence thin gas disk between the combustion chamber and the beginning of the rocket nozzle radiating energy to the interior downstream of the nozzle contour for a class of coaxial axisymmetric converging diverging rocket nozzles. The radiation view factors presented in this thesis for the projections which are blocked or shadowed through the throat radiating downstream to the contour have never been presented before in the literature It was found that the curvature of the function of the contour of the nozzle being either concave up or down and the slope of the first derivative being either positive or negative determined the values used for the transformation of the Stokes Theorem into terms of x, r (radius) and $f(x)$ for the evaluation of the line integral. The analytical solutions from the view factors of, for example, the interior of a combustion chamber, or any radiating heat source to a disk may then be applied to the solution of the view factor of the disk to the interior of the rocket nozzle contour presented here.

This modular building block type approach is what the author desires to allow the development of an interstellar matter antimatter rocket engine. The gases of this type of reaction shall approach those towards the speed of light, which shall involve a transport phenomena, which the author is looking forward to researching the solution.

TABLE OF CONTENTS

LIST OF TABLES

LIST OF FIGURES

CHAPTER I

MATHEMATICAL FORMULATION

The following procedure is employed to formulate the view factor between a disk and the interior of an arbitrary axisymmetric body.

1. The contour integral method [6, page 81-88] [2] [1]is used to derive the shape factor between a differential element and a disk.

2. An analytical expression for the view factor, $dF_{d-\delta r}$ is obtained from the disk to the interior of a differential conical ring, which is generated by rotating the above differential element around the axis passing through the center of the disk.

3. The above result is integrated along the interior surface of the axisymmetric body to give the view factor from a disk to the interior of a coaxial axisymmetric body. Details of mathematical formulation procedure follow.

1.1 View Factor From a Differential Planar Source to a Disk

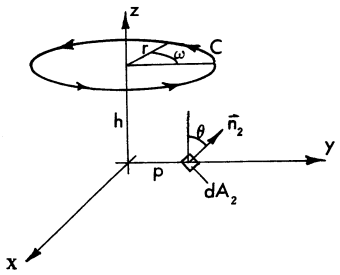

Figure 1: Differential Element with a full view and Normal in Quad I Radiating to Disk

This problem can be divided into two parts, namely, the disk is fully visible by the differential element and the disk is partially visible from the differential element in Figure 1 . The first case holds when the plane of the differential element does not intersect the disk, while the second case corresponds to the situation when dA_2 and the disk intersect.

Case la. The disk is fully visible by the element This case holds when the normal vector, $\vec{n}2$ points towards the II Quadrant with respect to itself plus $-\pi/2 \leq \theta \leq \pi/2$ and $\tan^{-1}\frac{h}{p-r} \leq \theta \leq \tan^{-1}\frac{h}{p+r}$ where r is the disk radius, h and p are the distance from the disk and differential element to the center of coordinates. The shape factor F_{dA_1-d} can be expressed as the sum of the contour integrals in the following manner [1].

$$F_{dA_1-d} = l_2 \oint_C \frac{(z_2-z_1)dy-(y_2-y_1)dz}{2\pi L^2} + m_2 \oint_C \frac{(x_2-x_1)dz-(z_2-z_1)dx}{2\pi L^2} + n_2 \oint_C \frac{(y_2-y_1)dx-(x_2-x_1)dy}{2\pi L^2} \quad (1.1)$$

Where C is the contour around the disk and 1_2, m_2 and n_2 are the direction

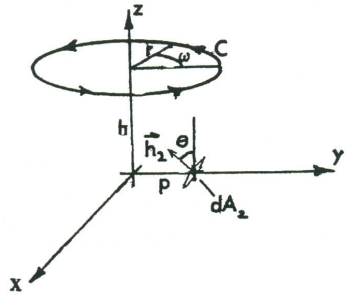

Figure 2: Differential Element with a full view and Normal in Quad 11 Radiating to Disk

cosines of the outward normal vector, $\vec{n}_2$

It can be seen from Figure 2 that $x_2 = 0, y_2 = P, z_2 = 0, x = r\sin\omega, y = r\cos\omega, z = h, 1_2 = 0, m_2 = -\sin(-\theta), n_2 = \cos(-\theta)$ and $L^2 = r^2\sin^2\omega + (p - r\cos\omega)^2 + h^2 = r^2 + p^2 + h^2 - 2pr\cos\omega$

$$F_{dA_1-d} = 0 - \sin(-\theta)\oint_C \frac{-(h-0)r\cos\omega d\omega}{2\pi(r^2+p^2+h^2-2pr\cos\omega)} + \cos(-\theta)\oint_C \frac{(r\cos\omega - p)r\cos\omega d\omega - (r\sin\omega - O)(-r\sin\omega d\omega)}{2\pi(r^2+p^2+h^2-2pr\cos\omega)} \quad (1.2)$$

$$F_{dA_1-d} = \cos(-\theta)\oint_C \frac{r^2 - pr\cos\omega d\omega}{2\pi(r^2+p^2+h^2-2pr\cos\omega)} - \sin(-\theta)\oint_C \frac{-hr\cos\omega d\omega}{2\pi(r^2+p^2+h^2-2pr\cos\omega)} \quad (1.3)$$

$$F_{dA_1-d} = \cos(-\theta)\int_0^{2\pi} \frac{r^2 - pr\cos\omega d\omega}{2\pi(r^2+p^2+h^2-2pr\cos\omega)} - \sin(-\theta)\int_0^{2\pi} \frac{-hr\cos\omega d\omega}{2\pi(r^2+p^2+h^2-2pr\cos\omega)} \quad (1.4)$$

and the result of this integration is as follows

$$F_{(dA_2-d)\text{RegionINormalQuadII}} = \frac{p\cos(\theta) + h\sin(\theta) + \frac{\sqrt{1-\frac{4pr}{h^2+(p+r)^2}}\left(-p\left(h^2+p^2-r^2\right)\cos(\theta) - h\left(h^2+p^2+r^2\right)\sin(\theta)\right)}{h^2+(p-r)^2}}{2p} \quad (1.5)$$

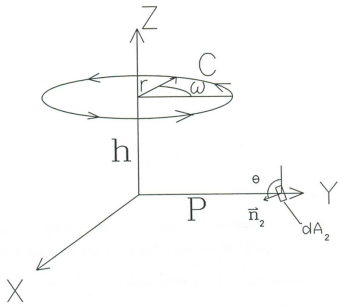

Figure 3: Differential Element with a full view and Normal in Quad III radiating to Disk

Case lb. The disk is fully visible by the element This case holds when the normal vector, $\vec{n}_2$ points towards Quadrant III with respect to itself plus $\pi/2 \leq \theta \leq \pi$ and $\tan^{-1}(h/(p-r)) \leq \theta \leq \tan^{-1}(h/(p+r))$ where r is the disk radius, h and p are the distance from the disk and differential element to the center at coordinates. The shape factor F_{dA_2-d} can be expressed as the sum of the contour integrals by following equation 1.1 as illustrated below. Where C is the contour around the disk and l_2, m_2 and n_2 are the direction cosines of the outward normal vector, $\vec{n}_2$

from Figure 3 that $x_2 = 0, y_2 = P, z_2 = 0, x = r\sin\omega, y = r\cos\omega, z = h, l_2 = 0, m_2 = -\sin(-\theta), n_2 = \cos(-\theta)$ and $L^2 = r^2\sin^2\omega + (p - r\cos\omega)^2 + h^2 = r^2 + p^2 + h^2 - 2pr\cos\omega$.

Substituting the above expressions into equation 1.1 yields.

$$F_{(dA_2-d)\text{RegionINormalQuadIII}} = \frac{-p\cos\theta + h\sin\theta + \frac{\sqrt{1-\frac{4pr}{h^2+(p+r)^2}}(p(h^2+p^2-r^2)\cos\theta - h(h^2+p^2+r^2)\sin\theta)}{h^2+(p-r)^2}}{2p} \quad (1.6)$$

Case IIa. The disk is partially visible by the element. This case holds when the normal vector $\vec{n}_2$, points towards the II Quadrant with respect to itself plus $0 \leq \theta \leq \frac{\pi}{2}$ and $\tan^{-1}\frac{h}{p+r} \leq \theta \leq \tan^{-1}\frac{h}{p-r}$. As shown in Figure 4, the differential element can only "see" a part of the disk (the shaded part in the top view of Figure 4).

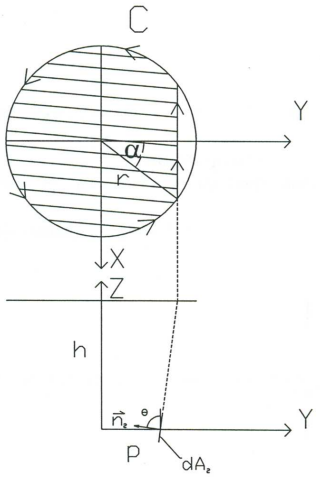

Figure 4: Differential Element with partial view and Normal in Quad II radiating to Disk

The corresponding contour C consists of a partial circle and a straight line. For the circle part, $x = r\sin\omega, y = r\cos\omega, Z = h, l_2 = 0, m_2 = -\sin\omega, n_2 = \cos\omega$

and $L^2 = r^2 + p^2 + h^2 2Pr\cos\omega$, with contour limits of integration as from $\omega = \cos^{-1}(\frac{h\cot\theta+p}{r})$ to $\omega = \pi$. For the straight line part,

$x = x, y = p + h\cot\theta, z = h, x_2 = 0, y_2 = p, z_2 = 0$ and $L^2 = x^2 + h^2\cot^2\theta + h^2$, with contour limits of integration as from $x = O$ to $x = \sqrt{r^2 - (h\cot\theta + p)^2}$. Substituting the above expressions into equation 1.1 and integrating yields

$$F_{(dA_2-d)\text{RegionIINormalQuadII}} =$$

$$+\frac{h\arctan(\frac{\sqrt{F1}}{\sqrt{G1}})\cos(\theta)\cot(\theta)}{\pi\sqrt{G1}}+\frac{h\arctan(\frac{\sqrt{F1}}{\sqrt{G1}})\sin(\theta)}{\pi\sqrt{G1}}+$$

$$+2\cos(\theta)(\frac{1}{4}-\frac{\arccos(A1)+\frac{2(H1)\arctan\, hypobolic\frac{(C1)\tan(\frac{\arccos(A1)}{2})}{\sqrt{D1}}}{\sqrt{D1}}}{4\pi})$$

$$-2\cos(\theta)(\frac{(H1)\sqrt{Sign(D1)}\sqrt{-(\frac{Sign(C1)^2}{Sign(D1)Sign(E1)^2})}Sign(E1)}{4\sqrt{D1}Sign(C1)})$$

$$-2\sin(\theta)(\frac{-(h(\arccos(A1)+\frac{2(B1)\arctan\, hyperbolic(\frac{(C1)\tan(\frac{\arccos(A1)}{2})}{\sqrt{D1}})}{\sqrt{D1}}))}{4P\pi})$$

$$-2\sin(\theta)(\frac{h(1-\frac{(B1)\sqrt{Sign(D1)}\sqrt{-(\frac{Sign(C1)^2}{Sign(D1)Sign(E1)^2})}Sign(E1)}{\sqrt{D1}Sign(C1)})}{4p})$$

where

$$A1=\frac{p+h\cot\theta}{r}$$

$$B1=h^2+p^2+r^2$$

$$C1=h^2+(p+r)^2$$

$$D1=-h^4-(p^2-r^2)^2-2h^2(p^2+r^2)$$

$$E1=\pi-\cos^{-1}(A1)$$

$$F1=-p^2+r^2-2hp\cot\theta-h^2\cot^2\theta$$

$$G1=h^2+h^2\cot^2\theta$$

$$H1=h^2+p^2-r^2$$

(1.7)

Case IIb. The disk is partially visible by the element This case holds when the normal vector, $\vec{n}_2$ points towards the III Quadrant with respect to itself plus $\pi/2\leq\theta\leq\pi$ and $\tan^{-1}\frac{h}{p+r}\leq\theta\leq\tan^{-1}\frac{h}{p-r}$. As shown in Figure 5, the differential element can only "see" a part of the disk (the shaded part in the top view of Figure 5).

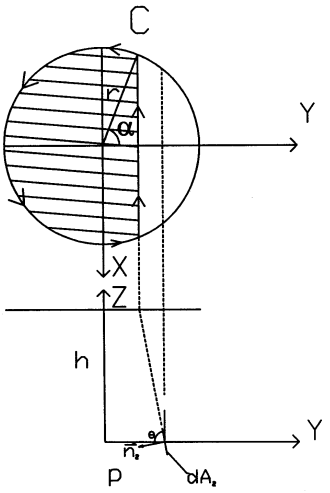

Figure 5: Differential Element with partial view and Normal in Quad III radiating to Disk

The corresponding contour C consists of a partial circle and a straight line. For the circle part, $x = r\sin\omega, y = r\cos\omega, z = h, l_2 = 0, m_2 = -\sin\theta, n_2 = -\cos\theta$ and $L^2 = r^2 + p^2 + h^2 - 2pr\cos\omega$ with contour limits of integration as from $\omega = \cos^{-1}((p - h\cot(\pi - \theta))/r)$ to $\omega = \pi$ .For the straight line part, $x = x, y = p + h\cot\theta, Z = h, x_2 = 0, y_2 = p, z_2 = 0$, and $L^2 = x^2 + h^2\cot^2\theta + h^2$, with contour limits of integration as from $x = 0$ to $x = \sqrt{r^2 - (p - h\cot(\pi - \theta))^2}$. Substituting the above expressions into equation 1.1 and integrating yields

$$F_{(dA_2-d)\text{RegionIINormalQuadIII}} =$$

$$-\frac{h\arctan(\frac{\sqrt{F2}}{\sqrt{G2}})\cos(\theta)\cot(\theta)}{\pi\sqrt{G2}}+\frac{h\arctan(\frac{\sqrt{F2}}{\sqrt{G2}})\sin(\theta)}{\pi\sqrt{G2}}$$

$$-2\cos(\theta)(\frac{1}{4}-\frac{\arccos(A2)+\frac{2(H2)\arctan hyperbolic(\frac{C2\tan(\frac{\arccos(A2)}{2})}{\sqrt{D2}})}{\sqrt{D2}}}{4\pi})$$

$$-2\cos(\theta)(\frac{H2\sqrt{Sign(D2)}\sqrt{-(\frac{Sign(C2)^2}{Sign(D2)Sign(E2)^2})}Sign(E2)}{4\sqrt{D2}Sign(C2)})$$

$$+2\sin(\theta)(\frac{h(\arccos(A2)+\frac{2(B2)\arctan hyperbolic(\frac{C2\tan(\frac{\arccos(A2)}{2})}{\sqrt{D2}})}{\sqrt{D2}})}{4p\pi})$$

$$-2\sin(\theta)(\frac{h(1-\frac{B2\sqrt{Sign(D2)}\sqrt{-(\frac{Sign(C2)^2}{Sign(D2)Sign(E2)^2})}Sign(E2)}{\sqrt{D2}Sign(C2)})}{4p})$$

where

$$A2=\frac{p+h\cot\theta}{r}$$

$$B2=h^2+p^2+r^2$$

$$C2=h^2+(p+r)^2$$

$$D2=-h^4-(p^2-r^2)^2-2h^2(p^2+r^2)=-(h^2+(p+r)^2)(h^2+(p-r)^2)$$

$$E2=\pi-\cos^{-1}(A2)$$

$$F2=-p^2+r^2-2hp\cot\theta-h^2\cot^2\theta=(r-p-h\cot\theta)(r+p+h\cot\theta)$$

$$G2=h^2+h^2\cot^2\theta=h^2/\sin^2\theta$$

$$H2=h^2+p^2-r^2$$

(1.8)

When

$0\le\theta\le\pi$ and $\tan^{-1}\frac{h}{p+r}\le\theta\le\tan^{-1}\frac{h}{p-r}$

Equation 1.5 through Equation 1.8 for the Radiation View Factors between

and disk and the interior of axisymmetric bodies are not yet available in the open literature. Figure 6 plots the view factors from the differential element to the disk versus θ with p as.a parameter when $H = 1$

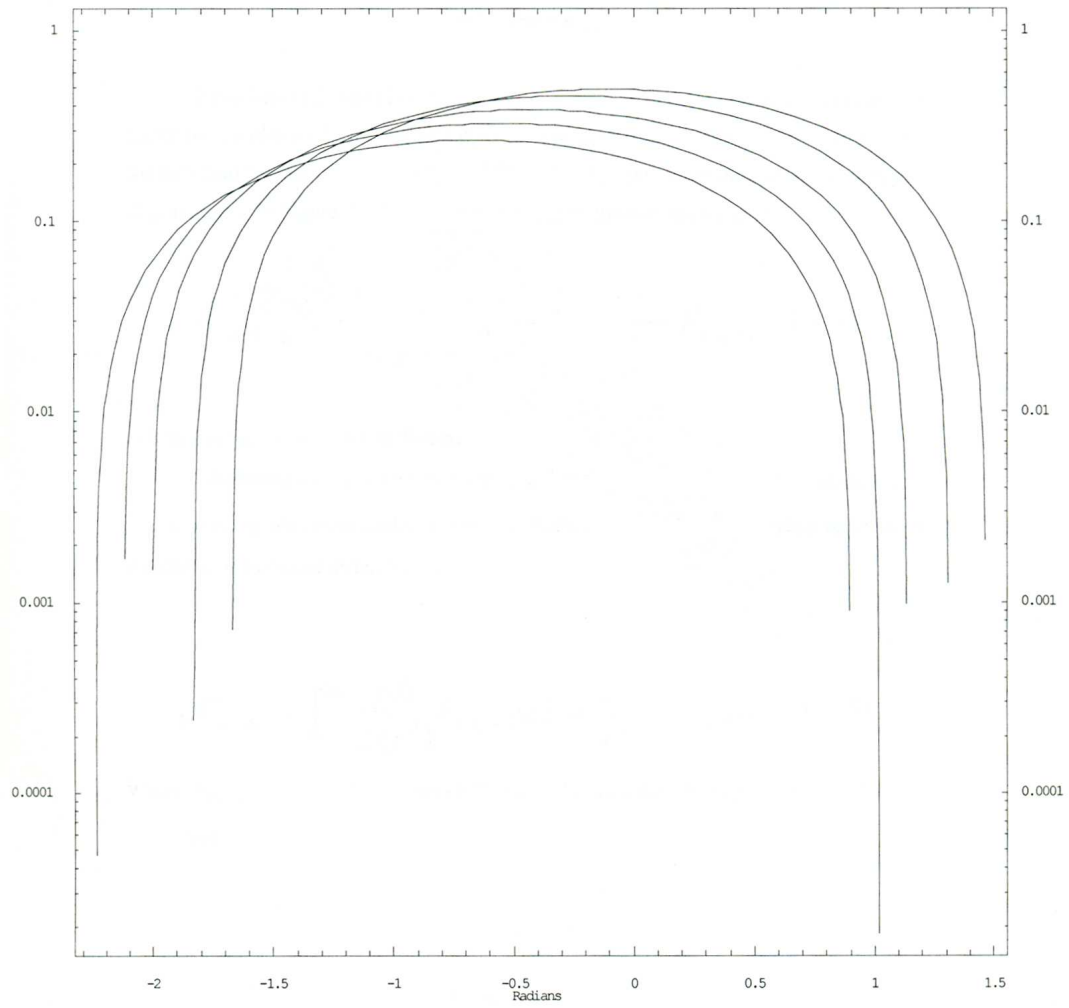

Figure 6: Graph of the radiation view factors of the differential element versus θ with p as parameter.

1.2 View Factor from A Disk to A Coaxial Differential Ring

Equation 1.5 through Equation 1.8 are employed to develop an expression for the geometry factor from a disk to the interior of a coaxial differential conical ring. We now consider the radiation between the disk and any differential element on the interior of the coaxial ring as shown in Figure7. The application of the reciprocal rule leads to

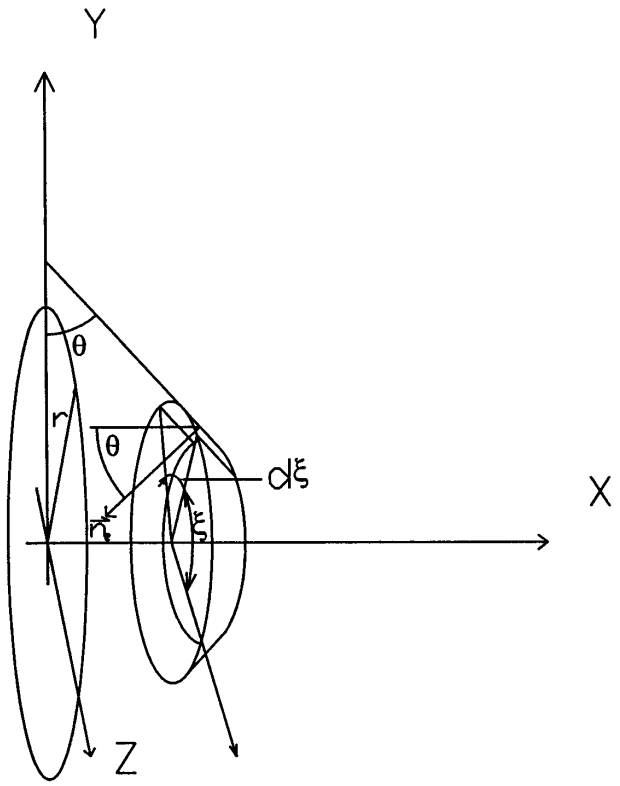

Figure 7: Disk radiating to interior of coaxial differential conical Ring 3D view

$$dF_{d-dA_2} = \frac{dA_2}{\pi r^2} F_{dA_2-d} = \frac{y d\xi ds}{\pi r^2} F_{dA_2-d} \tag{1.9}$$

Where y is the radius of the differential ring.

Integrating dF_{d-dA_2} with respect to ξ and noting that the F_{dA_2-d} is independent of Ixi due to the symmetrical configuration, we obtain an expression for the view factor from the disk to the coaxial differential ring as

$$dF_{d-\delta r} = \int_0^{2\pi} \frac{yds}{\pi r^2} F_{dA_2-d} d\xi = \frac{2y}{r^2} F_{dA_2-d} ds \tag{1.10}$$

Where F_{dA_2-d} is given by Equation 1.5 through Equation 1.8. Note that the expression for $dF_{d-\delta r}$ is in a closed form.

1.3 View Factor from a Disk to the Interior of a Coaxial Axisymmetric Body

Let the differential ring obtained from Equation 1.10 be a differential section of the interior of an axisymmetric body and let $y = f(x)$ be the function generator of this axisymmetric body (i.e., the axisymmetric body is generated from the rotation of $f(x)$ around the x-axis). Referring to Figure 8 we have

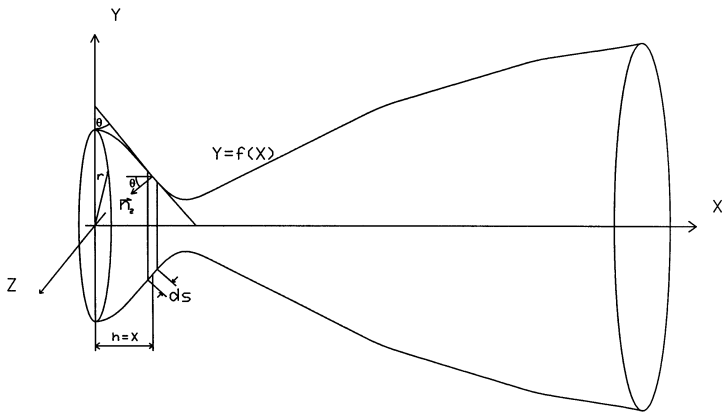

Figure 8: Nozzle 3D view

$$
\begin{aligned}
ds &= \sqrt{1 + [f'(x)]^2}dx \\
\theta &= \cot^{-1}[f'(x)] \\
\sin\theta &= \frac{1}{\sqrt{1 + [f'(x)]^2}} \\
\cos\theta &= \frac{f'(x)}{\sqrt{1 + [f'(x)]^2}} \\
p &= f(x) \\
h &= x
\end{aligned}
\tag{1.11}
$$

Substituting Equation 1.5 through Equation 1.8 into Equation 1.10 and making use of Equation 1.11 we obtain the following results for $dF_{d-\delta r}$ in terms of x, r and $f(x)$.

$$dF_{(d-\delta r)\text{RegionINormOuadII}} =$$

$$-(x + f(x)f'(x) - \frac{\sqrt{1 + \frac{4rf(x)}{x^2+(r-f(x))^2}}(x(r^2 + x^2 + f(x)^2) + f(x)(-r^2 + x^2 + f(x)^2)f'(x))}{r^2 + x^2 + 2rf(x) + f(x)^2})\frac{dx}{r^2} \tag{1.12}$$

$$dF_{(dA_2-\delta r)\text{RegionINormOuadII}} =$$

$$-\frac{\sqrt{1 + f'(x)^2}}{r^2}$$
$$(\frac{x}{\sqrt{1 + f'(x)^2}} + \frac{f(x)f'(x)}{\sqrt{1 + f'(x)^2}}$$
$$+ \frac{\sqrt{1 + \frac{4rf(x)}{x^2+(r-f(x))^2}}(-(\frac{x(r^2+x^2+f(x)^2)}{\sqrt{1+f'(x)^2}}) - \frac{f(x)(-r^2+x^2+f(x)^2)f'(x)}{\sqrt{1+f'(X)^2}})}{x^2 + (-r - f(x))^2})\frac{dx}{r^2} \tag{1.13}$$

$$dF_{(dA_2-\delta r)\text{RegionINormOuadIII}} =$$

$$(x - f(x)f'(x)$$
$$+ \frac{\sqrt{1 - \frac{4rf(x)}{x^2+(r+f(x))^2}}(-(x(r^2 + x^2 + f(x)^2)) + f(x)(-r^2 + x^2 + f(x)^2)f'(x))}{r^2 + x^2 - 2rf(x) + f(x)^2})\frac{dx}{r^2} \tag{1.14}$$

When $0 \leq x \leq x_i$

$dF_{(dA_2-\delta r)\text{RegionIInormOuadII}} =$

$$(2f(x)f1 - x(G22 - F22\,f2) + f(x)f'(x)(G22 - J22\,f2))\frac{dx}{\pi r A2}$$

where

$$f1 = \frac{\sqrt{A22}}{|x|}\arctan(\frac{\sqrt{H22}}{\sqrt{I22}})$$

$$f2 = 2\frac{\arctan hyperbolic(\frac{C22\tan(D22)}{\sqrt{E22}})}{\sqrt{E22}} + \pi\frac{\sqrt{Sign(E22)}\sqrt{-(\frac{Sign(C22)^2}{Sign(E22)Sign(G22)^2})}Sign(G22)}{\sqrt{E22}Sign(C22)}$$

$$A22 = 1 + f'(x)^2$$

$$B22 = \frac{f(x) + xf'(x)}{r}$$

$$C22 = x^2 + (r + f(x))^2$$

$$D22 = \frac{1}{2}\cos^{-1}(B22)$$

$$E22 = -x^4 - (f(x)^2 - r^2)^2 - 2x^2(f(x)^2 + r^2) = -(x^2 + (f(x) + r)^2)(x^2 + (f(x) - r)^2)$$

$$F22 = x^2 + f(x)^2 + r^2$$

$$G22 = \pi - \cos^{-1}(B22)$$

$$H22 = r^2 - f(x)^2 - 2xf(x)f'(x) - x^2f'(x)^2 = (r - f(x) - xf'(x))(r + f(x) + xf'(x))$$

$$I22 = x^2 + x^2f'(x)^2 = x^2A22$$

$$J22 = x^2 + f(x)^2 - r^2$$

(1.15)

$$dF_{(dA_2-\delta r)\text{RegionIInormOuadIII}} =$$

$$(2f(x)f1 - x(G23 - F23\,f2) + f(x)f'(x)(G23 - J23\,f2))\frac{dx}{\pi r A2}$$

where

$$f1 = \frac{\sqrt{A23}}{|x|}\arctan(\frac{\sqrt{H23}}{\sqrt{I23}})$$

$$f2 = 2\frac{\arctan\, hyperbolic(\frac{C23\tan(D23)}{\sqrt{E23}})}{\sqrt{E23}} + \pi\frac{\sqrt{Sign(E23)}\sqrt{-(\frac{Sign(C23)^2}{Sign(E23)Sign(G23)^2})}Sign(G23)}{\sqrt{E23}Sign(C23)}$$

$$A23 = 1 + f'(x)^2$$

$$B23 = \frac{f(x) + xf'(x)}{r}$$

$$C23 = x^2 + (r + f(x))^2$$

$$D23 = \frac{1}{2}\cos^{-1}(B23)$$

$$E23 = -x^4 - (f(x)^2 - r^2)^2 - 2x^2(f(x)^2 + r^2) = -(x^2 + (f(x) + r)^2)(x^2 + (f(x) - r)^2)$$

$$F23 = x^2 + f(x)^2 + r^2$$

$$G23 = \pi - \cos^{-1}(B23)$$

$$H23 = r^2 - f(x)^2 - 2xf(x)f'(x) - x^2f'(x)^2 = (r - f(x) - xf'(x))(r + f(x) + xf'(x))$$

$$I23 = x^2 + x^2f'(x)^2 = x^2A23$$

$$J23 = x^2 + f(x)^2 - r^2$$

(1.16)

To determine the configuration factor between the disk and the interior of a coaxial axisymmetric body, expressions given by Equation 1.12 through Equation 1.16 have to be integrated over the entire interior of the axisymmetric body. To do so we divide the interior of the axisymmetric body into the following three regions as illustrated in Figure 9.

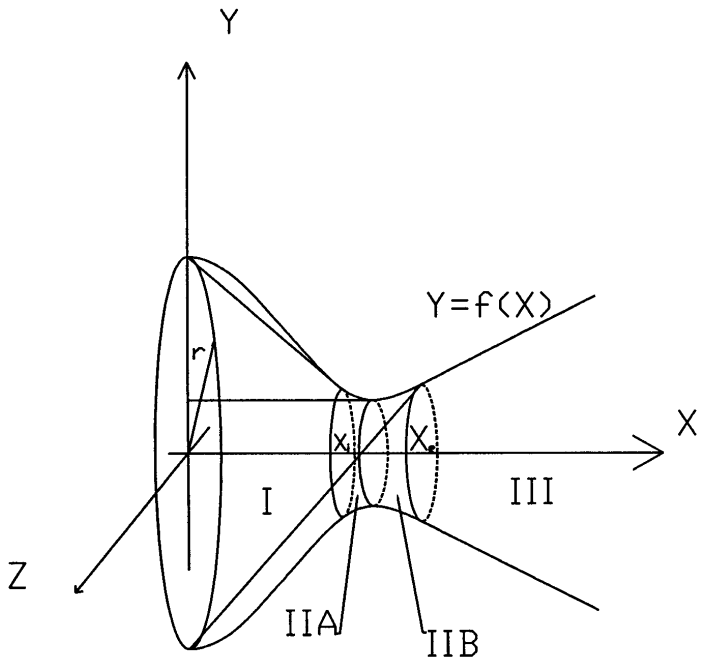

Figure 9: 3D view of a nozzle labeled Full and Partial view radiation sections

Region I. The region which can be seen from the disk but none of the tangent planes intersect the disk, i.e., $x_i \leq x \leq x_e$. portion of the interior of the axisymmetric body whose tangent planes always intersect the disk, i.e.,$x_i \leq x \leq x_e$. the interior of the axisymmetric body which cannot be seen by the disk, i.e., $x \geq x_e$.

Integrating

$dF_{d-\delta r}$ over the Regions I and II mentioned above yields the radiation shape factor from the disk to the entire interior of the axisymmetric body, $F_{d-\mathrm{ax}}$,

$$F_{d-\mathrm{ax}} = \int_0^{x_i} dF_{d-\delta r_{\mathrm{I}}} + \int_{x_i}^{x_e} dF_{d-\delta r_{\mathrm{II}}} = F_{d-\mathrm{I}} + F_{d-\mathrm{II}} \tag{1.17}$$

The first part of the integrals in Equation 1.17 is most unlikely to be explicitly integrated exactly as being an explicit definite integral so therefore a numerical integration may be used to solve $F_{d-\mathrm{I}}$ which is written in the following forms:

$$F_{(d-\mathrm{I})RegionINormQuadII} =$$

$$-\int_0^{x_i}(x+f(x)f'(x)-$$

$$\frac{\sqrt{1+\frac{4rf(x)}{x^2+(r-f(x))^2}}(x(r^2+x^2+f(x)^2)+f(x)(-r^2+x^2+f(x)^2)f'(x))}{r^2+x^2+2rf(x)+f(x)^2})\frac{dx}{r^2} \tag{1.18}$$

$$F_{(d-\mathrm{I})RegionINormQuadII} =$$

$$-\int_0^{x_i}\frac{2f(x)}{r^2}(\frac{1}{2f(x)}(\frac{x}{\sqrt{1+f'(x)^2}}+\frac{f(x)f'(x)}{\sqrt{1+f'(x)^2}}$$
$$+\frac{\sqrt{1+\frac{4rf(x)}{x^2+(r-f(x))^2}}(-(\frac{x(r^2+x^2+f(x)^2)}{\sqrt{1+f'(x)^2}})-\frac{f(x)(-r^2+x^2+f(x)^2)f'(x)}{\sqrt{1+f'(x)^2}})}{x^2+(-r-f(x))^2}))\sqrt{1+f'(x)^2}dx \tag{1.19}$$

$$F_{(d-\mathrm{I})RegionINormQuadIII} =$$

$$\int_0^{x_i}(x-f(x)f'(x)$$
$$+\frac{\sqrt{1-\frac{4rf(x)}{x^2+(r+f(x))^2}}(-(x(r^2+x^2+f(x)^2))+f(x)(-r^2+x^2+f(x)^2f'(x))}{r^2+x^2-2rf(x)+f(x)A2})\frac{dx}{r^2} \tag{1.20}$$

$$F_{(d-\mathrm{I})RegionINormQuadIII} =$$

$$\int_0^{x_i} \frac{2f(x)}{r^2}\frac{1}{2f(x)}\Big(\frac{x}{\sqrt{1+f'(x)^2}} - \frac{f(x)f'(x)}{\sqrt{1+f'(x)^2}} + \frac{\sqrt{1-\frac{4rf(x)}{x^2+(r+f(x))^2}}\Big(-\big(\frac{x(r^2+x^2+f(x)^2)}{\sqrt{1+f'(x)^2}}\big) + \frac{f(x)(-r^2+x^2+f(x)^2)f'(x)}{\sqrt{1+f'(x)^2}}\big)}{x^2+(-r+f(x))^2}\Big)\sqrt{1+f'(X)^2}dx \tag{1.21}$$

The second part of the integrals in Equation is most unlikely to be explicitly integrated exactly as being an explicit definite integral so therefore a numerical integration may be used to solve $F_{d-\mathrm{II}}$ which is written in the following forms:

$$F_{(d-\mathrm{II})RegionIINormQuadII} =$$

$$\int_{x_i}^{x_e} (2f(x)f1 - x(G22 - F22f2) + f(x)f'(x)(G22 - J22f2))\frac{dx}{\pi r^2}$$

where

$$f1 = \frac{\sqrt{A22}}{|x|}\arctan(\frac{\sqrt{H22}}{\sqrt{I22}})$$

$$f2 = 2\frac{ArcTanh(\frac{C22\tan(D22)}{\sqrt{E22}})}{\sqrt{E22}} + \pi\frac{\sqrt{Sign(E22)}\sqrt{-(\frac{Sign(C22)^2}{Sign(E22)Sign(G22)^2})}Sign(G22)}{\sqrt{E22}Sign(C22)}$$

$$A22 = 1 + f'(x)^2$$

$$B22 = \frac{f(x) + xf'(x)}{r}$$

$$C22 = X^2 + (r + f(x))^2$$

$$D22 = \frac{1}{2}\cos^{-1}(B22)$$

$$E22 = -x^4 - (f(x)^2 - r^2)^2 - 2x^2(f(x)^2 + r^2) = -(x^2 + (f(x) + r)^2)(x^2 + (f(x) - r)^2)$$

$$F22 = x^2 + f(X)^2 + r^2$$

$$G22 = \pi - \cos^{-1}(B22)$$

$$H22 = r^2 - f(x)^2 - 2xf(x)f'(x) - x^2f'(x)^2 = (r - f(x) - xf'(x))(r + f(x) + xf'(x))$$

$$I22 = x^2 + x^2f'(x)^2 = x^2A22$$

$$J22 = X^2 + f(x)^2 - r^2$$

(1.22)

$$F_{(d-\mathrm{II})RegionIINormQuadIII} =$$

$$\int_{x_i}^{x_e} (2f(x)f1 - x(G23 - F23f2) + f(x)f'(x)(G23 - J23f2))\frac{dx}{\pi r^2}$$

where

$$f1 = \frac{\sqrt{A23}}{|x|}\arctan(\frac{\sqrt{H23}}{\sqrt{I23}})$$

$$f2 = 2\frac{ArcTanh(\frac{C23\tan(D23)}{\sqrt{E23}})}{\sqrt{E23}} + \pi\frac{\sqrt{Sign(E23)}\sqrt{-(\frac{Sign(C23)^2}{Sign(E23)Sign(G23)^2})}Sign(G23)}{\sqrt{E23}Sign(C23)}$$

$$A23 = 1 + f'(x)^2$$

$$B23 = \frac{f(x) + xf'(x)}{r}$$

$$C23 = X^2 + (r + f(x))^2$$

$$D23 = \frac{1}{2}\cos^{-1}(B23)$$

$$E23 = -x^4 - (f(x)^2 - r^2)^2 - 2x^2(f(x)^2 + r^2) = -(x^2 + (f(x) + r)^2)(x^2 + (f(x) - r)^2)$$

$$F23 = x^2 + f(X)^2 + r^2$$

$$G23 = \pi - \cos^{-1}(B23)$$

$$H23 = r^2 - f(x)^2 - 2xf(x)f'(x) - x^2f'(x)^2 = (r - f(x) - xf'(x))(r + f(x) + xf'(x))$$

$$I23 = x^2 + x^2f'(x)^2 = x^2A23$$

$$J23 = X^2 + f(x)^2 - r^2$$

(1.23)

Referring to Figure 10 the integration limits in Equation 1.17 through Equation 1.23 can be obtained from the following Equation 1.24 and Equation 1.25:

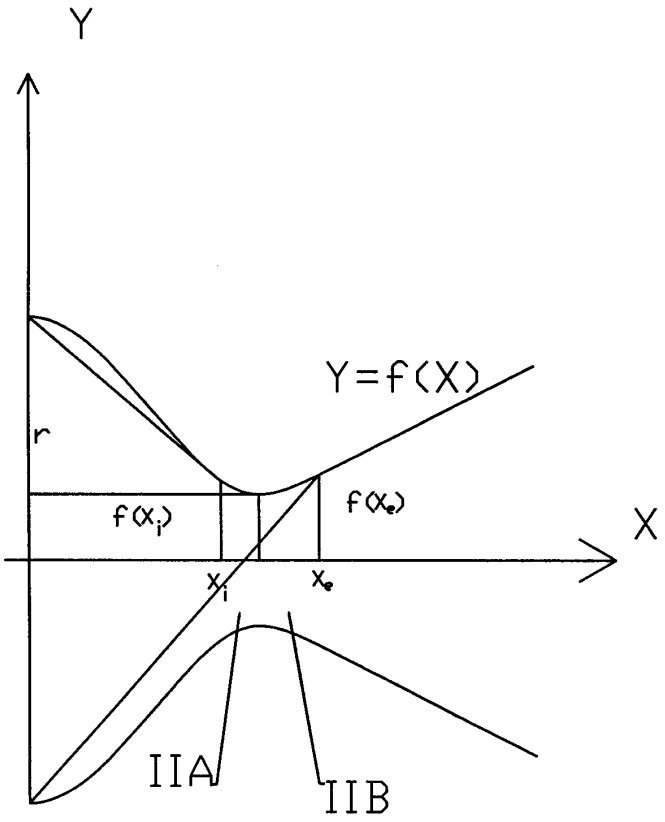

Figure 10: Limits of begining and end of Partial view factors Cross section y=f(x)

$$x_i f'(x_i) - f(x_i) = -r \tag{1.24}$$

$$-x_e f'(x_e) - f(x_i) = -r \tag{1.25}$$

CHAPTER II

MATHEMATICAL FORMULATION OF SHADOWING

The radiation of the differential area to the disk is shadowed by the throat section where only tangent lines continue their path as illustrated in the following Figure 11 through Figure 15 below.

$$F_{dA_1-d} = l_2 \oint_C \frac{(z_2 - z_1)dy - (y_2 - y_1)dz}{2\pi L^2} + m_2 \oint_C \frac{(x_2 - x_1)dz - (z_2 - z_1)dx}{2\pi L^2} + n_2 \oint_C \frac{(y_2 - y_1)dx - (x_2 - x_1)dy}{2\pi L^2} \quad (2.1)$$

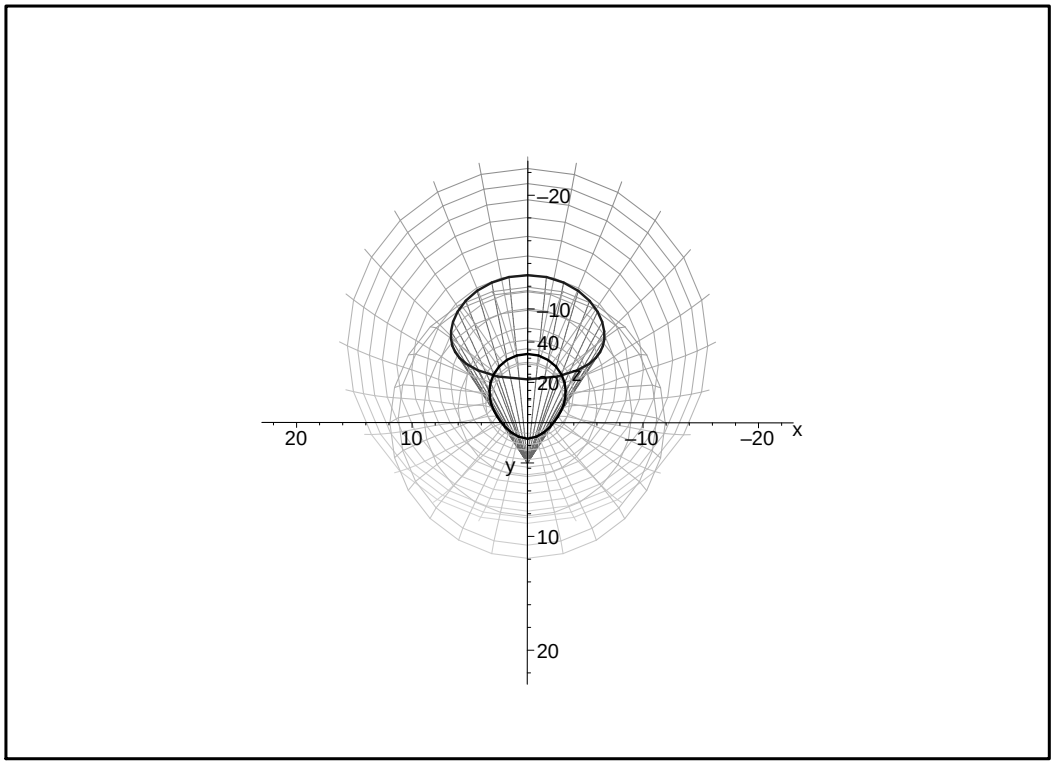

Figure 11: Shadowed projection through throat upon disk at zbegin=20

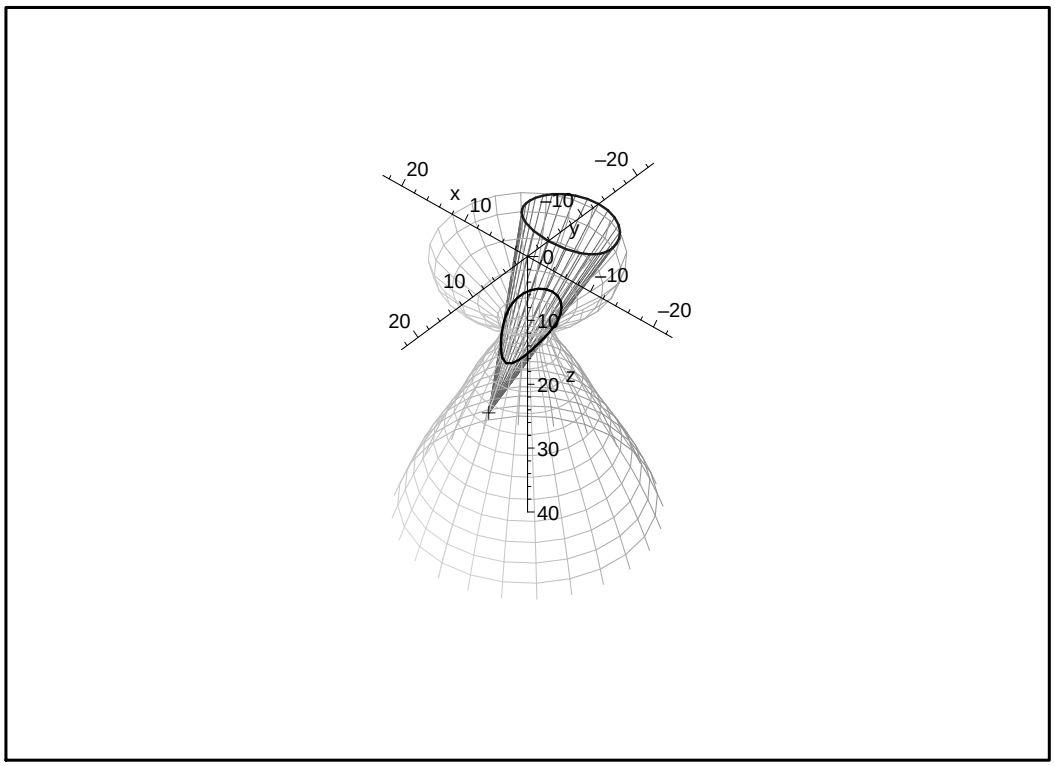

Figure 12: Shadowed projection through throat upon disk at zbegin=20

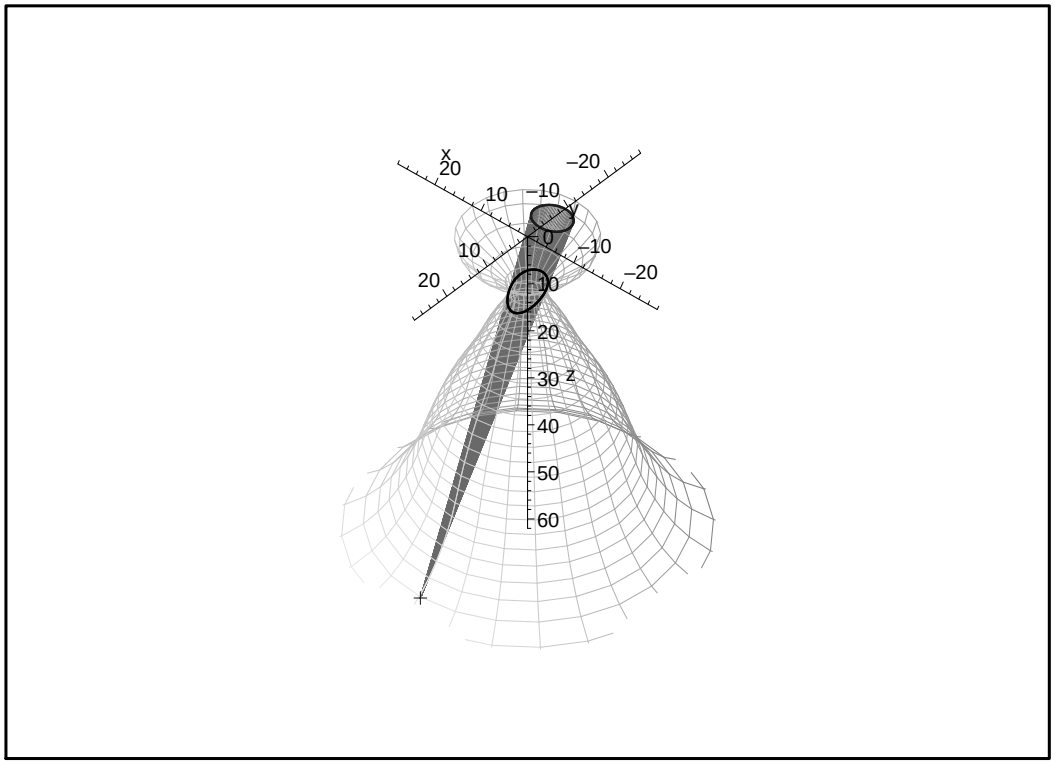

Figure 13: Shadowed projection through throat upon disk at zbegin=60

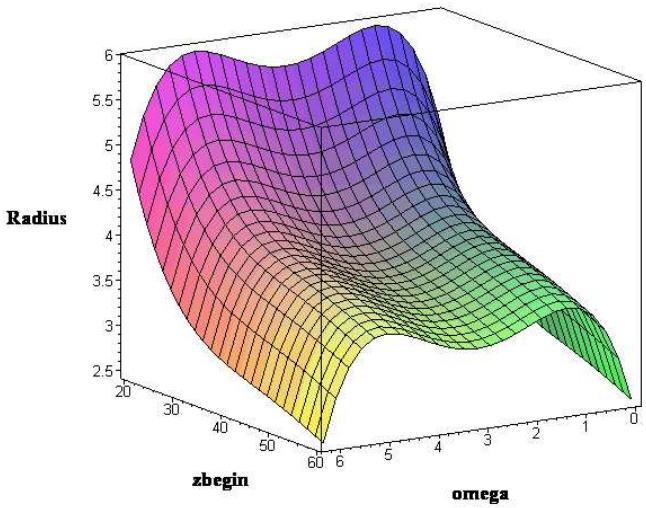

Figure 14: x=omega rotation around nonlinear cone axis, y=zbegin where the differential element, z=radius of curve projected upon the xy plane with center of curve being the function alpha which moves along x axis depending on zbegin position see alpha function in next figure

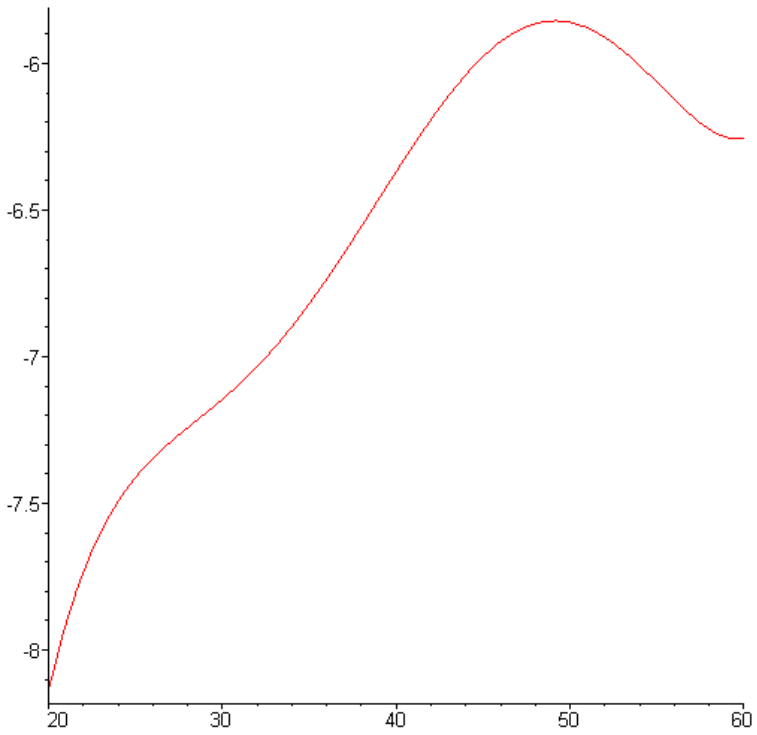

Figure 15: alpha function which is the center of the radius of xy projected plane curve vs. zbegin position

$$x_1 = P$$

$$Y_1 = 0$$

$$z_1 = 0$$

$$x_2 = \alpha + r\cos\omega$$

$$y_2 = r\sin\omega$$

$$z_2 = h$$

$$l_1 = \sin\theta$$

$$m_1 = 0$$

$$n_1 = \cos\theta$$

$$L^2 = ((((\alpha + (r\cos\omega)) - p)^2) + ((r\sin\omega)^2) + h^2))$$

$$dx_2 = (\partial_{z_1}\alpha + \partial_{z_1} r\cos\omega)dz_1 + (-r\sin\omega + \partial_\omega r\cos\omega)d\omega$$

$$dy_2 = (r\cos\omega + \partial_\omega r\sin\omega)d\omega + (\partial_{z_1} r\sin\omega)dz_1$$

$$dz_2 = 0$$

(2.2)

$$F_{dA_2-d} = \sin(\theta)\int_0^{2\pi} \frac{h((r\cos\omega) + ((\partial_\omega r)\sin\omega))d\omega}{(2\pi((((\alpha + (r\cos\omega)) - p)^2) + ((r\sin\omega)^2) + h^2))}$$
$$+\cos(\theta)\int_0^{2\pi} \frac{(((r\sin\omega)(((\partial_\omega r)\cos\omega) - r\sin\omega)) - (((\alpha + (r\cos\omega)) - p)(r\cos\omega + ((\partial_\omega r)\sin\omega))))d\omega}{(2\pi((((\alpha + (r\cos\omega)) - p)^2) + ((r\sin\omega)^2) + h^2))}$$

(2.3)

$$F_{dA_2-d} = \frac{-((p-\alpha)\left(h^2+(-p+r+\alpha)^2\right)\cos(\theta)+h\left(h^2+(-p+r+\alpha)^2\right)\sin(\theta))}{2\,(p-\alpha)\left(h^2+(-p+r+\alpha)^2\right)}$$
$$+\frac{\sqrt{\frac{h^2+(-p+r+\alpha)^2}{h^2+(p+r-\alpha)^2}}\left((p-\alpha)\left(h^2+p^2-r^2-2\,p\,\alpha+\alpha^2\right)\cos(\theta)+h\left(h^2+r^2+(p-\alpha)^2\right)\sin(\theta)\right)}{2\,(p-\alpha)\left(h^2+(-p+r+\alpha)^2\right)} \tag{2.4}$$

For an example of shadowing radiation view factor calculation, if we use a surface plot of the radius of projection upon the disk as illustrated in Figure 14 which center is from a function alpha that moves along the x axis as illustrated in Figure 15 where both function plots depend upon where the originating differential area source of radiation along the rocket contour at zbegin as illustrated in the Figure 11through Figure 13 We can take the equation of the surface plot and name it r and plug it in to Equation 2.3 along with the equation for alpha and integrate from 0 to 2π with respect to omega rotating around the nonlinear cones axis to end up with a result in terms of zbegin and thus therefore allow us to eliminate the need of the problem of the partial differential non linear tangent points curve rotated around the inside of the throat and simply have where the source of radiation starts and then projects upon the disk thus providing us for the first time no where to be found in the open literature with a radiation view factor from the differential area shadowed through the interior of a differential geometric surface of revolutions throat to a disk. which is now provide by the author of this thesis as illustrated in Equation 2.4.

Now then we can take the result in Equation 2.4 and plug it in to Equation 1.10 to provide us with the radiation view factor of the differential circular ring shadowed to the disk again no where available in the open literature.

Then we can take the result in the shadowed view factor for circular ring to disk and then plug it into Equation 1.17 and integrate along the entire interior contour of the axisymmetric differential geometric surface of revolution to then be provided

for the first time the shadowed radiation view factor from a disk of the combustion chamber to the interior contour of a rocket nozzle. No where to be found in the open literature.

Why do we need this shadowing view factor between the disk and the interior of rocket nozzle and Why is it so important? The answer is as follows, In order to get the temperature downstream past throat to properly cool the rocket nozzle at any point along its contour, this has been a problem since 1958 and which the first time in man kinds history which now has been solved by the author of this thesis.

CHAPTER III

RESULTS AND DISCUSSION

Based on the aforementioned general formulations, equations (1-10) - (1-13), the view factors from a disk to the interior of any converging diverging rocket nozzle is investigated. The first illustration is with a straight line cone nozzle with the following data in Figure 16.

please look at Figure 16 Figure 17 The example rocket nozzle in this thesis which is the original problem rocket contour from 1958 by Robbins [5, 3, 4] at NASA is from 0 to 69 but as illustrate by Robbins they could only calculate a view factor up to where the z axis length of 14.3765 with a view factor of 0.9798436 as illustrated in Table I. Robins [5, 3, 4] and all other authors considered the rest of the heat transfer with the view factors from 0.9798436 to 1.0 to be considered as negligible but from z=14.3765 where the view factor is 0.9798436 to z=69 along the z axis of the rocket nozzle is where the view factor approaches or near a view factor value of 1.0 past the invisible range of around z=14.3765 to around z=15.34 where then the shadowing occurs is a very important section where compressible flow shock waves occur near the exit of the rocket nozzle and where temperatures could not be calculated before

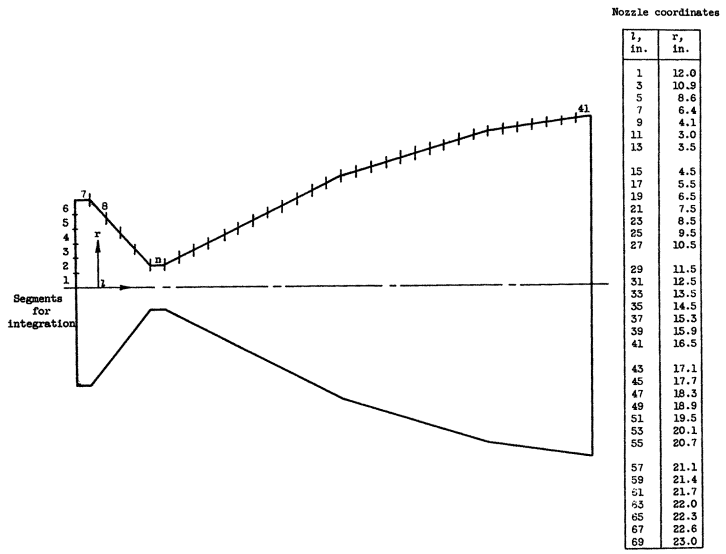

Nozzle coordinates

l, in.	r, in.
1	12.0
3	10.9
5	8.6
7	6.4
9	4.1
11	3.0
13	3.5
15	4.5
17	5.5
19	6.5
21	7.5
23	8.5
25	9.5
27	10.5
29	11.5
31	12.5
33	13.5
35	14.5
37	15.3
39	15.9
41	16.5
43	17.1
45	17.7
47	18.3
49	18.9
51	19.5
53	20.1
55	20.7
57	21.1
59	21.4
61	21.7
63	22.0
65	22.3
67	22.6
69	23.0

Figure 16: Nozzle Geometry. Wall Thickness and Material, 0.020-Inch Stainless Steel; Chamber Temperature, 4680 Degrees R; Throat Diameter, 6 Inches; Ratio of Inlet Area To Throat Area, 16; Ratio of Exit Area to Throat Area, 59; Nozzle Axial Length,70 Inches

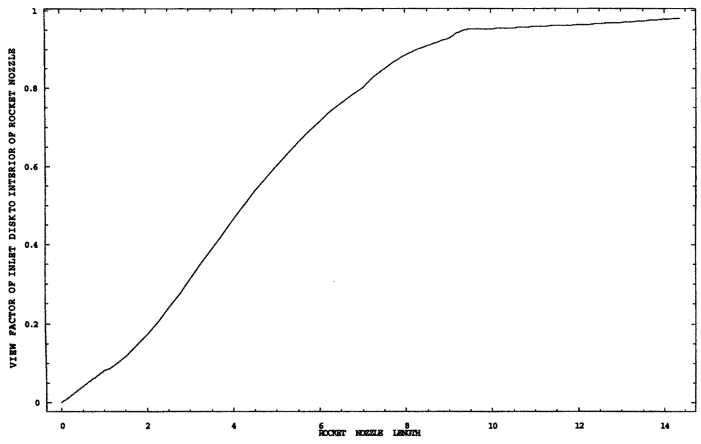

Figure 17: Graph of Radiation View Factor of Disk to Interior of Rocket Nozzle Length

DISTANCE FROM INLET DISK ALONG LENGTH AXIS OF THE INTERIOR OF ROCKET NOZZLE CONTOUR	VIEW FACTOR OF DISK TO INTERIOR OF THE ROCKET NOZZLE CONTOUR FOR SPECIFIED DISTANCE ALONG LENGTH OF ROCKET NOZZLE AXIS	TOTAL VIEW FACTOR OF DISK TO THE INTERIOR OF ROCKET NOZZLE CONTOUR FROM THE BEGINNING OF THE ROCKET NOZZLE TO THE END OF THE SPECIFIED DISTANCE ALONG THE ROCKET NOZZLE LENGTH AXIS	TOTAL VIEW FACTOR OF DISK TO THE INTERIOR OF ROCKET NOZZLE CONTOUR FROM THE BEGINNING OF THE ROCKET NOZZLE TO THE END OF THE SPECIFIED DISTANCE ALONG THE ROCKET NOZZLE LENGTH AXIS USING $F_{\text{disk1-interior}} = 1 - F_{\text{disk1-disk2}}$
0-1	0.0799334	0.0799334	0.0799334
1-7	0.720457	0.8003904	0.800408
7-9	0.126896	0.92728	0.927339
9-9.47039	0.0250127	0.9522991	0.952352
9.47037-11	0.0062562	0.9585553	0.966566
11-14.3765	0.0212883	0.9798436	

Table I: Table of Radiation View Factors of Disk to Interior of Rocket Nozzle up to Invisible Section Range14.3765-15.34which is before where the Shadowing Phenomena occurs Range15.34-69

because the previous authors did not have the shadowing View factors that the author of this thesis have now provided today in his lords year of 2008. Nor did the previous authors have the Super computers or the symbolic integration capabilities of Mathematica or Maple which we now have today that we needed in order to have done the shadowing view factors.

For the sake of a rough estimation of the view Factor of a disk to the interior of a converging diverging rocket nozzle a View Factor of an enclosure around a disk is considered to be near the value of 1 with considering the exit of the nozzle which is out to the environment. Now if the View Factor of a disk at the beginning of the rocket nozzle to the disk at the throat of a converging diverging nozzle value is calculated, and then that value is subtracted from 1 which is the value of a disk with an enclosure above, then this value therefore provides a rough estimate of the view factor of a disk to the interior of a rocket nozzle which then may be obtained for a rough comparison of the contour line integration values calculated in this paper. For example the view factor of the inlet disk to the throat disk and interior of the given

nozzle in Figure 16 is illustrated and calculated below.

$$r_1 = 12.0$$

$$r_2 = 3.0$$

$$h = 11.0$$

$$R_1 = \frac{r_1}{h} = 1.09091$$

$$R_2 = \frac{r_2}{h} = 0.272727$$

$$X = 1 + \frac{1 + {R_2}^2}{{R_1}^2} = 1.90278$$

$$F_{\text{INLETDISK-THROATDISK}} = \frac{1}{2}[X - \sqrt{X^2 - 4(\frac{R_2}{R_1})^2}] = 0.0334342$$

$$F_{\text{INLETDISK-INTERIOROFROCKETNOZZLE}} = 1 - F_{\text{INLETDISK-THROATDISK}} = 0.966566$$

(3.1)

It has been illustrated that a comparison of the rough estimate of the view factor of a disk to the interior of a rocket nozzle being of a value of 0.97 for a distance of 11 inches along length axis of the nozzle from the beginning of the rocket nozzle contour to the throat is within reason of the calculated contour integral view factor of 0.96. The total view factor including all partial views of the disk along the rocket nozzle contour has been found to 0.98 these values are illustrated in Figure 17. Mathematica 5.0 and 6.0 were found to have a bug in the integrations and only Mathematica 4.0 could do the integrations Maple 11 could not simplify the view factors like Mathematica could and this made it a big problem for the supercomputer to do parallel cluster nodes and batch files had to be done. for the shadowing view factors Wolfram is presently working on the bug in the integral development department.

CHAPTER IV

CONCLUDING REMARKS

The shadowing view factors were found to be very small within the .02 range as expected and the author shall be updating these values and new shadowing View Factors in a web site at www.csuohio.edu/engineering/mce by June 4th, 2008 or the author may be reached at mark_murad@hotmail.com for all updates from Wolfram and Maple supercomputer results with the new method that Professor John Oprea and the author are working on. The Future View Factors must be parameterized for the Differential Geometrists

BIBLIOGRAPHY

[1] J. Hammad, Khaled. Radiative heat transfer in rocket thrust chambers and nozzles. *Masters Of Science Thesis, Manhattan College, Manhattan , New York*, (1), 1989.

[2] M. Naraghi. Radiation configuration factors between disks and axisymmetric bodies. *Masters Of Science Thesis, University of Akron, Akron, Ohio*, (1), 1981.

[3] H. Robbins, William. An analysis of thermal radiation heat transfer in a nuclear-rocket nozzle. *NASA*, Technical Note(D-586), 1961.

[4] H. Robbins, William. Analysis, feasibility,and wall temperature distribution of a radiation cooled nuclear rocket nozzle. *NASA*, Technical Note(D-878), 1962.

[5] H. Robbins, William. An analysis of nuclear-rocket nozzle cooling. *NASA*, Technical Note(D-482), 1962.

[6] E. Sparrow. A new and simpler formulation for radiative angle factors. *Journal of Heat Transfer, Trans ASME*, 85(2):81–88, 1963.

APPENDIX

APPENDIX A

MATHEMATICA AND MAPLE PROGRAMS

```
Rocket Nozzle Geometry
> restart:
> with(plots):with(LinearAlgebra):
>
> EFG := proc(X)
> local Xu,Xv,E,F,G;
> Xu := <diff(X[1],u),diff(X[2],u),diff(X[3],u)>;
> Xv := <diff(X[1],v),diff(X[2],v),diff(X[3],v)>;
> E := DotProduct(Xu,Xu,conjugate=false);
> F := DotProduct(Xu,Xv,conjugate=false);
> G := DotProduct(Xv,Xv,conjugate=false);
> simplify([E,F,G]);
> end:
> UN := proc(X)
```

```
> local Xu,Xv,Z,s;
> Xu := <diff(X[1],u),diff(X[2],u),diff(X[3],u)>;
> Xv := <diff(X[1],v),diff(X[2],v),diff(X[3],v)>;
> Z := CrossProduct(Xu,Xv);
> s:=VectorNorm(Z,Euclidean,conjugate=false);
>  simplify(<Z[1]/s|Z[2]/s|Z[3]/s>,sqrt,trig,symbolic);
> end:
> lmn := proc(X)
> local Xu,Xv,Xuu,Xuv,Xvv,U,l,m,n;
> Xu := <diff(X[1],u),diff(X[2],u),diff(X[3],u)>;
> Xv := <diff(X[1],v),diff(X[2],v),diff(X[3],v)>;
> Xuu := <diff(Xu[1],u),diff(Xu[2],u),diff(Xu[3],u)>;
> Xuv := <diff(Xu[1],v),diff(Xu[2],v),diff(Xu[3],v)>;
> Xvv := <diff(Xv[1],v),diff(Xv[2],v),diff(Xv[3],v)>;
> U := UN(X);
> l := DotProduct(U,Xuu,conjugate=false);
> m := DotProduct(U,Xuv,conjugate=false);
> n := DotProduct(U,Xvv,conjugate=false);
> simplify([l,m,n],sqrt,trig,symbolic);
> end:
```

Finally we can calculate Gauss curvature K as follows.

```
> GK := proc(X)
> local E,F,G,l,m,n,S,T;
> S := EFG(X);
> T := lmn(X);
> E := S[1];
> F := S[2];
> G := S[3];
```

```
> l := T[1];
> m := T[2];
> n := T[3];
> simplify((l*n-m^2)/(E*G-F^2),sqrt,trig,symbolic);
> end:
The procedure below finds the z-values z_k where the
line from a given z-value z_i is tangent to the rnoz
surface of revolution. The procedure now handles z_k's
both above and below the throat. The procedure plots
the surface with style = wireframe. To see the surface
better, switch to style=patch.
> rocketnoz2:=proc(f,g,z_i,N,u0,u1,x0,x1,y0,y1,z0,z1,zz,p,q)
> local L,K,F,G,i,sol,V,pl1,pl2,surf,minn,line_at_minn,ww:
> L:=[];
> F:=t->eval(f,u=t);
> G:=t->eval(g,u=t);
> minn:=F(zz);
> print(‘Gauss curvature at z_i is‘,evalf(eval(GK(<F(u)*cos(v),
F(u)*sin(v),G(u)>),{u=z_i,v=0})));
> K:=[];
> for i from 0 to N do
> sol:=fsolve(-F(z_i)*diff(G(s),s)*cos(i/N*2*Pi)+
F(s)*diff(G(s),s)
> -G(s)*diff(F(s),s)+G(z_i)*diff(F(s),s)=0,
s=zz-p..zz+q);
> if type(sol,numeric)=true then
> if sol<=zz then
> ww:=fsolve(G(z_i)+w*(G(sol)-G(z_i))=zz,w=0..1);
```

```
> if type(ww,numeric)=true then
> line_at_minn:=map(evalf,
(<F(z_i)+ww*(F(sol)*cos(i/N*2*Pi)-F(z_i)),
ww*F(sol)*sin(i/N*2*Pi),
> G(z_i)+ww*(G(sol)-G(z_i))>));
> V:=Norm(<line_at_minn[1],line_at_minn[2]>,
Euclidean,
conjugate=false);
> if V <= minn then L:=[op(L),[i/N*2*Pi,sol]];
> K:=[op(K),[F(sol)*cos(i/N*2*Pi),
F(sol)*sin(i/N*2*Pi),G(sol)]];
> #print(evalf(DotProduct
(eval(UN(<F(u)*cos(v),F(u)*sin(v),G(u)>),
{u=sol,v=i/N*2*Pi}),
> #(<F(sol)*cos(i/N*2*Pi),
F(sol)*sin(i/N*2*Pi),G(sol)> -
<F(z_i),0,G(z_i)>)/
> #VectorNorm((<F(sol)*cos(i/N*2*Pi),
F(sol)*sin(i/N*2*Pi),G(sol)> - <F(z_i),0,G(z_i)>),
> #Euclidean,conjugate=false),conjugate=false)))
> fi;
> fi;
> if type(ww,numeric)=false then next; fi;
> fi;
> if zz<sol then L:=[op(L),[i/N*2*Pi,sol]];
> K:=[op(K),[F(sol)*cos(i/N*2*Pi),
F(sol)*sin(i/N*2*Pi),G(sol)]];
> fi;
```

```
> fi;
> od;
> print(L);
> pl1:=pointplot3d([[F(z_i),0,G(z_i)]],color=blue,thickness=3,
symbol=cross,symbolsize=28):
> pl2:=pointplot3d(K,connect=true,color=black,thickness=3,
symbol=cross,
symbolsize=28):
> surf:=plot3d(<F(u)*cos(v),F(u)*sin(v),G(u)>,u=u0..u1,
v=0..2*Pi,shading=XY,
grid=[30,25],
> style=wireframe):
> display(pl1,pl2,surf,scaling=constrained,
view=[x0..x1,y0..y1,z0..z1]);
> end:
> rocketnoz_disk_proj:=proc(f,g,z_i,N,zz,p,q)
> local K,F,G,i,sol,V,pl1,pl2,surf,minn,line_at_minn,
ww,tt,disk_pl:
> F:=t->eval(f,u=t);
> G:=t->eval(g,u=t);
> minn:=F(zz);
> K:=[];
> for i from 0 to N do
> sol:=fsolve(-F(z_i)*diff(G(s),s)*cos(i/N*2*Pi)+F(s)*diff(G(s),s)
> -G(s)*diff(F(s),s)+G(z_i)*diff(F(s),s)=0,s=zz-p..zz+q);
> if type(sol,numeric)=true then
> if sol<=zz then
> ww:=fsolve(G(z_i)+w*(G(sol)-G(z_i))=zz,w=0..1);
```

```
> if type(ww,numeric)=true then
> line_at_minn:=map(evalf,(<F(z_i)+ww*(F(sol)*cos(i/N*2*Pi)-F(z_i)),
ww*F(sol)*sin(i/N*2*Pi),
> G(z_i)+ww*(G(sol)-G(z_i))>));
> V:=Norm(<line_at_minn[1],line_at_minn[2]>,Euclidean,
conjugate=false);
> if V <= minn then
> tt:=fsolve(G(z_i)+t*(G(sol)-G(z_i))=0,t);
> K:=[op(K),map(evalf,[F(z_i)+tt*(F(sol)*cos(i/N*2*Pi)-F(z_i)),
tt*F(sol)*sin(i/N*2*Pi),
> G(z_i)+tt*(G(sol)-G(z_i))])];
> fi;
> fi;
> if type(ww,numeric)=false then next; fi;
> fi;
> if zz<sol then
> tt:=fsolve(G(z_i)+t*(G(sol)-G(z_i))=0,t);
> K:=[op(K),map(evalf,[F(z_i)+tt*(F(sol)*cos(i/N*2*Pi)-F(z_i)),
tt*F(sol)*sin(i/N*2*Pi),
> G(z_i)+tt*(G(sol)-G(z_i))])];
> fi;
> fi;
> od;
> disk_pl:=pointplot3d(K,connect=true,color=blue,thickness=3,
symbol=cross,symbolsize=28):
> display(disk_pl,scaling=constrained,orientation=[0,0]);
> end:
> rocketnoz_with_proj:=proc(f,g,z_i,N,u0,u1,x0,x1,
```

```
y0,y1,z0,z1,zz,p,q)
> local K,J,F,G,i,sol,V,pl1,pl2,surf,minn,
line_at_minn,ww,tt,disk_pl:
> F:=t->eval(f,u=t);
> G:=t->eval(g,u=t);
> minn:=F(zz);
> K:=[];
> J:=[];
> for i from 0 to N do
> sol:=fsolve(-F(z_i)*diff(G(s),s)*cos(i/N*2*Pi)+F(s)*diff(G(s),s)
> -G(s)*diff(F(s),s)+G(z_i)*diff(F(s),s)=0,s=zz-p..zz+q);
> if type(sol,numeric)=true then
> if sol<=zz then
> ww:=fsolve(G(z_i)+w*(G(sol)-G(z_i))=zz,w=0..1);
> if type(ww,numeric)=true then
> line_at_minn:=map(evalf,(<F(z_i)+ww*(F(sol)*cos(i/N*2*Pi)
-F(z_i)),
ww*F(sol)*sin(i/N*2*Pi),
> G(z_i)+ww*(G(sol)-G(z_i))>));
> V:=Norm(<line_at_minn[1],line_at_minn[2]>,Euclidean,
conjugate=false);
> if V <= minn then
> tt:=fsolve(G(z_i)+t*(G(sol)-G(z_i))=0,t);
> J:=[op(J),map(evalf,[F(z_i)+tt*(F(sol)*cos(i/N*2*Pi)
-F(z_i)),
tt*F(sol)*sin(i/N*2*Pi),
> G(z_i)+tt*(G(sol)-G(z_i))])];
> K:=[op(K),[F(sol)*cos(i/N*2*Pi),F(sol)*sin(i/N*2*Pi),
```

```
G(sol)]];
> fi;
> fi;
> if type(ww,numeric)=false then next; fi;
> fi;
> if zz<sol then
> tt:=fsolve(G(z_i)+t*(G(sol)-G(z_i))=0,t);
> J:=[op(J),map(evalf,[F(z_i)+tt*(F(sol)*cos(i/N*2*Pi)
-F(z_i)),
tt*F(sol)*sin(i/N*2*Pi),
> G(z_i)+tt*(G(sol)-G(z_i))])];
> K:=[op(K),[F(sol)*cos(i/N*2*Pi),F(sol)*sin(i/N*2*Pi),
G(sol)]];
> fi;
> fi;
> od;
> pl1:=pointplot3d([[F(z_i),0,G(z_i)]],color=blue,
thickness=3,symbol=cross
,symbolsize=28):
> pl2:=pointplot3d(K,connect=true,color=black,
thickness=3,symbol=cross,
symbolsize=28):
> disk_pl:=pointplot3d(J,color=blue,thickness=3,
connect=true,symbol=cross,
symbolsize=32):
> surf:=plot3d(<F(u)*cos(v),F(u)*sin(v),G(u)>,
u=u0..u1,
v=0..2*Pi,shading=XY,
```

```
grid=[30,25],
> style=wireframe):
> display(pl1,pl2,disk_pl,surf,scaling=constrained,
view=[x0..x1,y0..y1,z0..z1]);
> end:
>
> rocketnoz_with_projlines:=
proc(f,g,z_i,N,u0,u1,x0,x1,y0,y1,z0,z1,zz,p,q,
theta,phi)
> local K,J,F,G,L,M,i,sol,V,aa,pl1,pl2,p13,surf,minn,
line_at_minn,ww,tt,disk_pl:
> F:=t->eval(f,u=t);
> G:=t->eval(g,u=t);
> minn:=F(zz);
> K:=[];
> J:=[];
> L:=[];
> M:=[];
> for i from 0 to N do
> sol:=fsolve(-F(z_i)*diff(G(s),s)*cos(i/N*2*Pi)+
F(s)*diff(G(s),s)
> -G(s)*diff(F(s),s)+G(z_i)*diff(F(s),s)=0,
s=zz-p..zz+q);
> if type(sol,numeric)=true then
> if sol<=zz then
> ww:=fsolve(G(z_i)+w*(G(sol)-G(z_i))=zz,w=0..1);
> if type(ww,numeric)=true then
> line_at_minn:=map(evalf,(<F(z_i)+
```

```
ww*(F(sol)*cos(i/N*2*Pi)-F(z_i)),
ww*F(sol)*sin(i/N*2*Pi),
> G(z_i)+ww*(G(sol)-G(z_i))>));
> V:=Norm(<line_at_minn[1],line_at_minn[2]>,
Euclidean,conjugate=false);
> if V <= minn then
> tt:=fsolve(G(z_i)+t*(G(sol)-G(z_i))=0,t);
> J:=[op(J),map(evalf,[F(z_i)+
tt*(F(sol)*cos(i/N*2*Pi)-F(z_i)),
tt*F(sol)*sin(i/N*2*Pi),
> G(z_i)+tt*(G(sol)-G(z_i))])];
> if i=0 then
> M:=[op(M),map(evalf,[F(z_i)+
tt*(F(sol)*cos(i/N*2*Pi)-F(z_i)),
tt*F(sol)*sin(i/N*2*Pi),
> G(z_i)+tt*(G(sol)-G(z_i))])] fi;
> if i=N/2 then
> M:=[op(M),map(evalf,[F(z_i)+
tt*(F(sol)*cos(i/N*2*Pi)-F(z_i)),
tt*F(sol)*sin(i/N*2*Pi),
> G(z_i)+tt*(G(sol)-G(z_i))])] fi;
> L:=[op(L),spacecurve([F(z_i)+s*(tt*(F(sol)*cos(i/N*2*Pi)
-F(z_i))),
s*(tt*F(sol)*sin(i/N*2*Pi)),
> (1-s)*G(z_i)],s=0..1,color=magenta)];
> K:=[op(K),[F(sol)*cos(i/N*2*Pi),F(sol)*sin(i/N*2*Pi),
G(sol)]];
> fi;
```

```
> fi;
> if type(ww,numeric)=false then next; fi;
> fi;
> if zz<sol then
> tt:=fsolve(G(z_i)+t*(G(sol)-G(z_i))=0,t);
> J:=[op(J),map(evalf,[F(z_i)+tt*(F(sol)*cos(i/N*2*Pi)
-F(z_i)),
tt*F(sol)*sin(i/N*2*Pi),
> G(z_i)+tt*(G(sol)-G(z_i))])];
> if i=0 then
> M:=[op(M),map(evalf,[F(z_i)+tt*(F(sol)*cos(i/N*2*Pi)
-F(z_i)),
tt*F(sol)*sin(i/N*2*Pi),
> G(z_i)+tt*(G(sol)-G(z_i))])] fi;
> if i=N/2 then
> M:=[op(M),map(evalf,[F(z_i)+tt*(F(sol)*cos(i/N*2*Pi)-F(z_i)),
tt*F(sol)*sin(i/N*2*Pi),
> G(z_i)+tt*(G(sol)-G(z_i))])] fi;
> L:=[op(L),spacecurve([F(z_i)+
s*(tt*(F(sol)*cos(i/N*2*Pi)-F(z_i))),
s*(tt*F(sol)*sin(i/N*2*Pi)),
> (1-s)*G(z_i),s=0..1],color=magenta)];
> K:=[op(K),[F(sol)*cos(i/N*2*Pi),
F(sol)*sin(i/N*2*Pi),G(sol)]];
> fi;
> fi;
> od;
> aa:=(M[1]+M[2])/2;
```

```
> print(‘The center of the projected curve is‘,aa);
> M:=[op(M),aa];
> print(‘The radius at omega=0 and omega=Pi are‘,M);
> pl1:=pointplot3d([[F(z_i),0,G(z_i)]],color=blue,
thickness=3,symbol=cross,
symbolsize=28):
> pl2:=pointplot3d(K,connect=true,color=black,
thickness=3,symbol=cross,
symbolsize=28):
> p13:=pointplot3d(M,connect=false,color=red,
symbol=cross,symbolsize=28);
> disk_pl:=pointplot3d(J,color=blue,thickness=3,
connect=true,symbol=cross,
symbolsize=32):
> surf:=plot3d(<F(u)*cos(v),F(u)*sin(v),G(u)>,
u=u0..u1,v=0..2*Pi,shading=XY,
grid=[30,25],
> style=wireframe):
> display(pl1,pl2,p13,disk_pl,surf,L,scaling=constrained,
view=[x0..x1,y0..y1,z0..z1],orientation=
> [theta,phi],axes=boxed,labels=[x,y,z],
labelfont=[TIMES, BOLD, 14],
resolution=1000);
> end:
>
> a(0):= 14.57090740:
> a(1):= 8.175351173:
> a(2):= 2.146354487:
```

```
> a(3):= -3.16176960:
> a(4):= 1.557809867:
> a(5):= -0.22956536:
> a(6):= -0.44950961:
> a(7):= 0.653013519:
> a(8):= -0.40905088:
> a(9):= 0.247331332:
> a(10):= -0.04046052:
> a(11):= -0.18397363:
> a(12):= 0.184463347:
> a(13):= -0.04796984:
> a(14):= -0.03453818:
> a(15):= 0.075301420:
> a(16):= -0.08041342:
>
> [seq([x, ChebyshevT(3,x)],x = -2 .. 2)];
> h := proc (x, n) options operator, arrow;
 sum(a(i)*ChebyshevT(i,.2898550725e-1*x-1),i = 0 .. n) end proc;
> rnoz:=expand(h(u,16));
> plot(rnoz,u=0..69,scaling=constrained);
> minimize(rnoz,u=0..15);
> fsolve(rnoz=3.02778568,u=10..12);
OK, I'm taking z_i = 60 and checking 100 points around the circle.
 The M is gone now and the interval where Maple looks for a
  numerical solution to the equation using fsolve is given by
   the throat z, called zz, and the final two inputs p and q.
    Interval is zz-p..zz+q.
> rocketnoz2(rnoz,u,60,100,0,69,-5,5,-5,5,7,20,11.41365589,
```

```
2.5,3);
> rocketnoz2(rnoz,u,60,100,0,69,-30,30,-30,30,0,69,
11.41365589,2.5,3);
> rocketnoz2(rnoz,u,43,100,0,69,-5,5,-5,5,7,20,
11.41365589,2.5,3);
> rocketnoz2(rnoz,u,30,50,0,69,-23,23,-23,23,0,40,
11.43730691,2.5,3);
> rocketnoz2(rnoz,u,20,30,0,69,-23,23,-23,23,0,40,
11.43730691,3.5,3);
> rocketnoz2(rnoz,u,20,30,0,30,-23,23,-23,23,0,40,
11.43730691,3.5,3);
> rocketnoz2(rnoz,u,13,60,0,69,-23,23,-23,23,0,40,
11.43730691,5.515,1.5);
> rocketnoz_disk_proj(rnoz,u,60,100,11.41365589,2.5,3);
> rocketnoz_disk_proj(rnoz,u,43,100,11.41365589,2.5,3);
> rocketnoz_with_proj(rnoz,u,60,100,0,69,-15,15,-15,
15,-0.1,20,11.41365589,2.5,3);

> rocketnoz_with_proj(rnoz,u,43,100,0,69,-15,15,-15,
15,-0.1,20,11.41365589,2.5,3);
> rocketnoz_with_proj(rnoz,u,20,30,0,69,-23,23,-23,23,
-0.1,40,11.43730691,3.5,3);
>
> rocketnoz_with_projlines(rnoz,u,60,30,0,69,-28,28,
-28,28,-0.1,62,11.41365589,
2.5,3,-117,-126);
> rocketnoz_with_projlines(rnoz,u,20,30,0,69,-23,23,
-23,23,-0.1,62,11.43730691,
```

```
3.5,3,-117,-126);



>

>
```